Reports of NAS RA
ՀՀ ԳԱԱ Զեկույցներ
NATIONAL ACADEMY OF SCIENCES OF THE REPUBLIC OF ARMENIA
ՀԱՅԱՍՏԱՆԻ ՀԱՆՐԱՊԵՏՈՒԹՅԱՆ ԳԻՏՈՒԹՅՈՒՆՆԵՐԻ ԱԶԳԱՅԻՆ ԱԿԱԴԵՄԻԱ

2026 **Volume 126** **Issue 1** **Article No. 5**

Category: Chemistry
Type of Paper: Original Research Article
Received: October 31, 2025, **Revised:** February 2, 2026, **Accepted:** February 3, 2026
Published: March 2, 2026

DOI: 10.54503/0321-1339-2026.126.1-5

Study of Various Aspects of the Mechanism of Cα-Alkylation of α-Amino Acids under Phase-Transfer Salen Catalysis Conditions

Anna S. Tovmasyan[1,*], Anna F. Mkrtchyan[1,2], Ashot S. Saghyan[1,2]

[1]Scientific and Production Center "Armbiotechnology" NAS RA, 14 Gyurjyan Str., Yerevan 0056, Armenia
[2]Yerevan State University, 1 Alex Manoogian Str., Yerevan 0025, Armenia

[*]Correspondence: anna.tovmasyan1@edu.isec.am

Abstract

The stereodifferentiating ability of salen complexes of Cu(II), Ni(II), and Zn(II) ions in Cα-alkylation reactions of amino acids as phase-transfer catalysts (PTC) has been investigated. We found that substituents in the 3-position of the aromatic ring of the salicylidene moiety of the complexes have a particularly strong effect on catalytic activity. The highest efficiency was observed for the 3-methoxy-substituted salen complex of the Zn (II) — ee > 90%. DFT calculations showed that the stereodifferentiating ability of the catalyst depends on the ratio of propeller-like and cross-like conformational structures of dimeric binuclear salen complex molecules in the alkylation transition state. It was demonstrated that propeller-like conformational isomers, which predominate in the dimeric binuclear structure of 3-allyl-substituted salen complexes, correspond to the catalytically inactive form and inhibit asymmetric catalysis. In contrast, cross-like isomers, which dominate in the dimeric binuclear structure of 3-methoxy-substituted salen complexes, ensure high stereodifferentiating activity and promote asymmetric catalysis. The DFT calculation data correlates clearly with the experimental results.

Keywords: phase transfer catalysis, asymmetric catalysis, salen complexes, alkylation, amino acids

1. Introduction

α-Amino acids are an important class of physiologically and pharmacologically active compounds. The demand for amino acids is steadily increasing due to their wide use in biotechnology, medicine, pharmaceutical and food industries, and other fields of science and technology, among which non-proteinogenic α-amino acids occupy a special place [1, 2]. The synthesis of non-proteinogenic α-amino acids is also in high demand due to their wide application in synthetic chemistry and chemistry of materials [3–9]. The development of efficient and straightforward methods for the synthesis of enantiomerically enriched non-proteinogenic α-amino acids is an extremely important task, since they are successfully used as irreversible enzyme inhibitors in numerous biomedical applications [10–12]. Among non-proteinogenic amino acids, various α, α-disubstituted amino acids — both in isolated form and as part of peptides — exhibit potential pharmacological activity [13–17]. One of the simple methods for synthesizing non-physiological α-amino acids is α-C(sp^3)–H alkylation of α-amino acids or their derivatives. However, only a few examples have been described, including the works of Zhaon [18], Yamamoto [19], and Yazaki and Ohshima [20, 21], which require the use of catalysts and

additives. On the other hand, numerous methods for the catalytic asymmetric synthesis of unnatural amino acids have been described, including hydrogenation of olefins and imines [22, 23], electrophilic amination of enolates [24, 25], electrophilic alkylation of glycine derivatives [26], and nucleophilic addition to α-imino esters [27]. In practice, chiral phase-transfer catalysts such as derivatives of cinchonine, TADDOL, NOBIN, and the Maruoka and Lygo catalysts have been successfully applied for the preparation of enantiomerically enriched non-proteinogenic amino acids [28]. Chiral salen complexes of transition metal ions Cu(II) and Ni(II), have also shown relatively high catalytic activity in phase-transfer asymmetric alkylation reactions of amino acid enolates [29].

2. Results and Discussion

We investigated the influence of substituents on the salicylaldehyde moiety of the complexes and the benzylidene amino acid substrates on the stereodifferentiating ability of the catalyst, with the aim of developing the most efficient catalytic system for the asymmetric synthesis of α-amino acids. To this end, numerous salen complexes of Cu(II), Ni(II) and Zn(II) ions, derived from the Schiff Base of chiral cyclohexyldiamine and substituted salicylaldehides, containing various substituents in different positions of the aromatic ring of the salicylaldehyde moiety were synthesized: methyl, allyl, *tert*-butyl, methoxy, ethoxy groups (Figure 1) [30]. As an analog of the O'Donnell substrate, the Schiff bases of the *iso*-propyl ester of aminoacids and substituted benzaldehydes were synthesized.

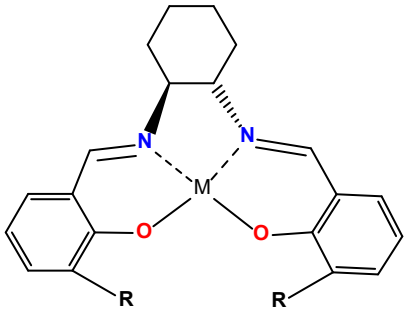

M=Cu, R=H (**1**)
M=Cu, R=OCH3(**2**)
M=Cu, R=Allyl(**3**)
M=Zn, R=H(**4**)
M=Zn, R=Allyl(**5**)
M=Zn, R=OCH3(**6**)
M=Ni, R=H(**7**)
M=Ni, R=Allyl(**8**)
M=Ni, R=OCH3(**9**)

Figure 1. Schematic structure of the complexes explored in this work.

To the best of our knowledge, most of these compounds were synthesized for the first time, in particular, all zinc salen complexes, fluorine-containing substrates and others. As a model reaction for evaluating the catalytic ability of the complexes, the alkylation of unsubstituted alanine substrate with benzyl bromide was chosen (Scheme 1).

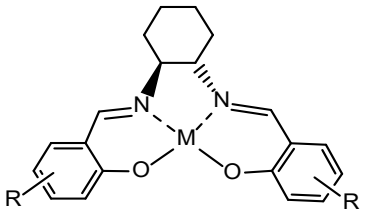

M= Cu(II), Ni(II), Zn(II)

R=Me, t-Bu, Allyl, MeO, EtO

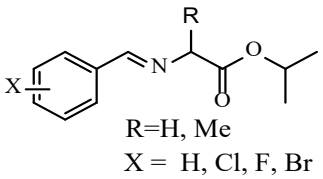

R=H, Me
X = H, Cl, F, Br

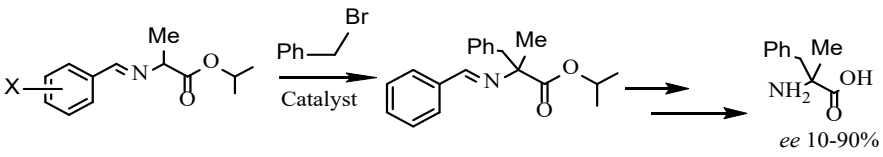

ee 10-90%

Scheme 1. Asymmetric alkylation of amino acid enolates under PTC with benzyl bromide.

The obtained results indicated that the synthesized complexes exhibit high catalytic activity, and for some complexes the enantiomeric excess of products reaches 90%. However, it was evident that the substituents in position 3 of the salicylaldehyde moiety have a particularly strong influence on the catalytic activity of salen complexes. Therefore, in subsequent experiments, we focused on salen complexes containing allylic and methoxy groups at position 3 of the salicylaldehyde moiety. For comparison, unsubstituted salen complexes of the same ions were also investigated [31] (Figure 2).

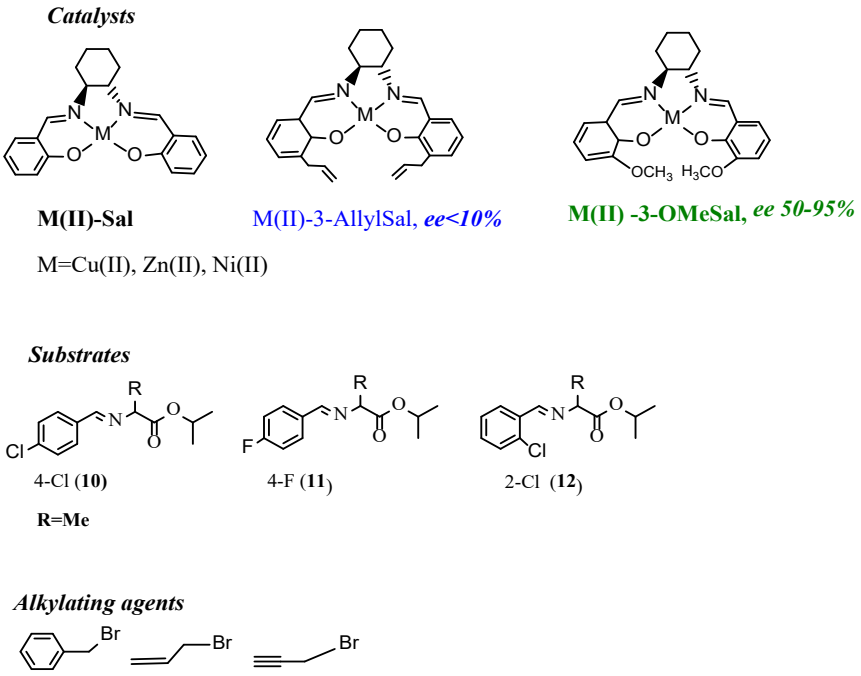

Figure 2. The structures of the salen complexes, amino acid substrates and alkylating agents.

As amino acid substrates, *o*-chlorine, *p*-chlorine and *p*-fluorine-substituted benzylidene derivatives were investigated, as an alkylating agent, benzyl bromide, allyl bromide and propargyl bromide were used. The results in the case of allylation reaction of alanine substrates are summarized in the Table 1.

Table 1. Conversion rates (c.r.) and enantiomeric excesses (ee) for the Cα-alkylation of substrates 10–12 with allyl bromide using PTC.

Catalyst	Substrate **10** *c.r. (%)**	*ee (%)***	Substrate **11** *c.r. (%)*	*ee (%)*	Substrate **12** *c.r. (%)*	*ee (%)*
1	80	74	55	32	85	70
2	10	<5	16	10	10	<5
3	**90**	**87**	**60**	**34**	**94**	**88**
4	10	<5	11	<5	10	<5
5	**15**	**10**	**20**	**12**	**10**	**<5**
6	95	90	75	54	95	93
7	45	56	34	22	64	58
8	**10**	**0**	**10**	**<5**	**10**	**0**
9	50	58	25	16	75	66

**- Conversion rates (c.r.) were determined by NMR spectroscopy*
***- Enantiomeric excesses (ee) were determined by chiral HPLC analysis of isolated products.*
The reactions were carried out using allyl bromide as the alkylating agent. Values reported as '<5' indicate enantiomeric excess below the reliable detection limit.

The obtained data showed that all complexes containing an allyl group at the 3-position of salicylaldehyde moiety in all alkylation reactions provide low stereoselectivity, not more than the 10% enantiomeric excess of the products, regardless of the nature of the alkylating agent and substrate. The opposite picture is observed in the case of salen complexes, containing a methoxy group at position 3 of the salicylaldehyde fragment. Practically in all alkylation reactions these complexes showed high stereo differentiation ability, regardless of the nature of the substrate and the alkylating agent. The most effective was the 3-methoxy-substituted zinc ion complex, which provides on average 90% enantiomeric excess of alkylated products.

The observed trends are summarized in the allylation reactions are presented in the Figure 3. Notably in the series of unsubstituted salen complexes, the catalytic activity of metal ions decreases in the following order: copper complexes are the most active ones, followed by nickel and then zinc complexes. In addition, transitioning from unsubstituted salen complexes to 3-allyl-substituted complexes leads to a significant inhibition of the catalytic activity.

In contrast, the transition from unsubstituted complexes to 3-methoxy-substituted complexes leads to increase of the catalytic activity. In series of these complexes the catalytic activity of metal ions decreases in the following order: zinc complexes are the most active – *ee 94%*, followed by copper complexes – *ee 87%* and then nickel complexes – *ee 58%.* These results indicate that strong increase in catalytic activity is observed in the case of zinc ion complexes.

In the series of substrates, efficiency decreases in the following order: ortho-chlorine, then para-chlorine and para-fluorine-substituted substrates.

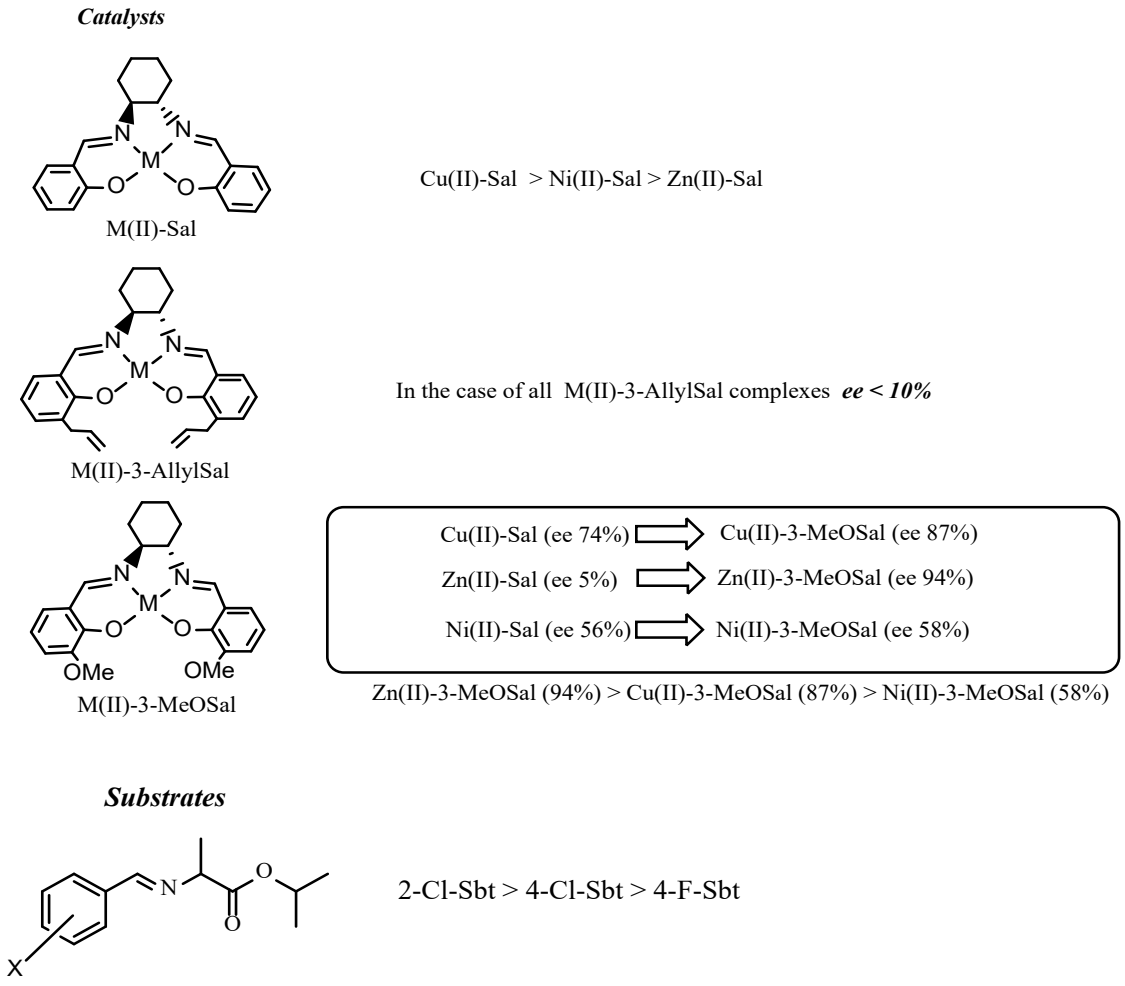

Figure 3. The identified patterns observed in the allylation reactions.

Summarizing the results, we can state that the introduction of an allyl group into position 3 of the salicylaldehyde moiety inhibits the catalytic activity of the complexes, whereas the introduction of a methoxy group at the same position, on the contrary, stimulates asymmetric catalysis.

An explanation for this phenomenon can be found based on the hypothetical model of the alkylation reaction mechanism proposed by Y.N. Belokon and M. North. [32, 33] (Figure 4).

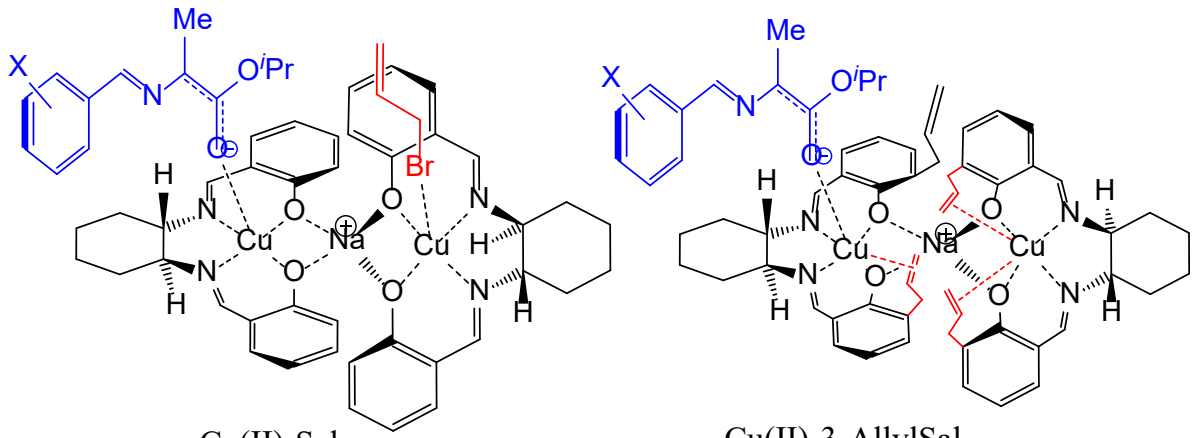

Figure 4. The proposed structure of the dimeric binuclear complex-catalyst in the transition state of alkylation: **a)** unsubstituted salicylidene complex; **b)** 3-allylsalicylidene complex.

According to this mechanism, in the transition state of alkylation, the catalyst takes part in the form of a dimeric binuclear derivative, which is formed due to additional coordination of oxygen atoms of the salen part of the complexes with the sodium ion. In the formed dimeric structure, both transition metal ions are coordinated to the ionized substrate and the alkylating agent. Their interaction occurs on a single coordination plane of the dimeric complex (Figure 4). This represents an active catalytic state.

To evaluate the experimental data, a conformational analysis of binuclear dimeric molecules formed from mononuclear salen complexes in the transition state of alkylation was performed using DFT calculations. For this purpose, changes in Gibbs free energy and Hirschfeld charges concentrated on the transition metal ions were determined (see Table 2), as well as the distance between the central transition metal ions during the dimerization of the complexes.

Table 2. Changes in electronic energy (ΔE) and Gibbs free energy (ΔG) during the formation of a binuclear structure from two mononuclear molecules.

	Zn(II)-H	**Zn(II)-OMe**	**Zn(II)-Allyl**	**Cu(II)-H**	**Cu(II)-OMe**	**Cu(II)-Allyl**
Δ***E***	-129.66	-182.24	-178.47	35.82	-14.38	3.44
Δ***G***	-56.55	-103.31	-94.94	102.05	69.02	87.86

DFT calculations showed that the Gibbs free energy of unsubstituted complexes of Cu(II), Ni(II), and Zn(II) ions is significantly higher than that of their 3-allyl-substituted analogs.

To evaluate the contribution of allyl fragment coordination to the transition metal ion, a conformational analysis of the resulting binuclear complex was performed [34].

Two dynamically stable conformers were identified: in one of them three out of four allyl fragments are coordinated to the transition metal ions, while in the other, only one out of four possible allyl fragments is coordinated (Figure 4b). This indicates that in solution, the conformation with coordinated allyl fragments predominates significantly, thereby hindering further reaction progress, which is supported by experimental data on reagent conversion.

The chemical nature of such allyl fragment coordination is also confirmed by the calculated Hirshfeld charges concentrated on the transition metal ions [35].

For example, in zinc complexes the charge increases from +0.40 to +0.48 upon dissociation of the allyl fragment, and in copper complexes from +0.20 to +0.24. Based on previously published studies, asymmetric alkylation of enolates catalyzed by a salen complex proceeds via an asynchronous S_N2-type reaction with the primary role of the catalyst being to enhance the nucleophilicity of the enolate [36].

This explains why the enantiomeric excess decreases when moving from Cu(II) to Zn(II) complexes, as the overall charge of the metal ion is reduced.

However, within the series of salicylidene Zn(II) complexes, the following phenomenon is observed. In case of the unsubstituted and 3-allyl-substituted Zn(II) complexes, the hypothesis holds true, as the asymmetric yield is much lower than that of other complexes.

But in the case of the 3-methoxy-substituted Zn(II) complex, the enantiomeric yield is high and exceeds that of all other complexes. Based on some observations from the work of Kostakis, we propose that the introduction of a methoxy group at the 3-position of the aromatic ring of the salicylaldehyde fragment in the metal complex enhances the rigidity of the intramolecular structure of the bimetallic derivative due to additional coordination with the sodium ion, thereby promoting asymmetric induction [37] (Figure 5).

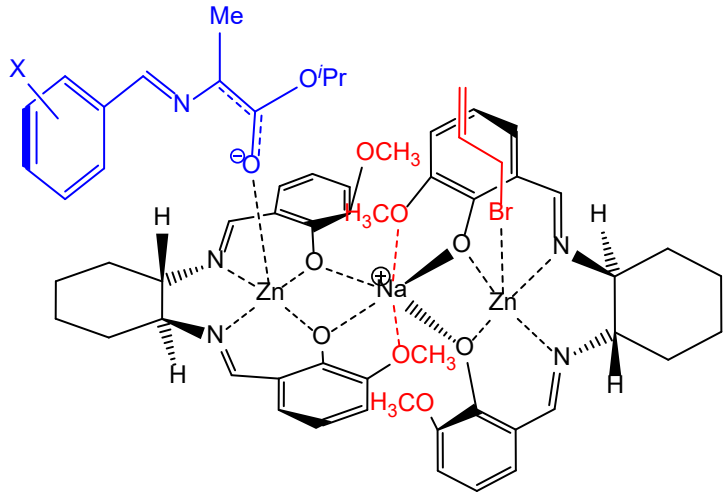

Figure 5. Possible intramolecular stabilization of the dimeric structure of the 3-methoxy-substituted Zn(II) salen complex in the transition state of alkylation.

Based on the analysis of DFT calculation data, it might be concluded that during the formation of dimeric complexes from monomeric salen complexes, the dimeric molecules are in the form of two conformational isomeric structures, Propeller-like structure and Cross-like structure (Figure 6).

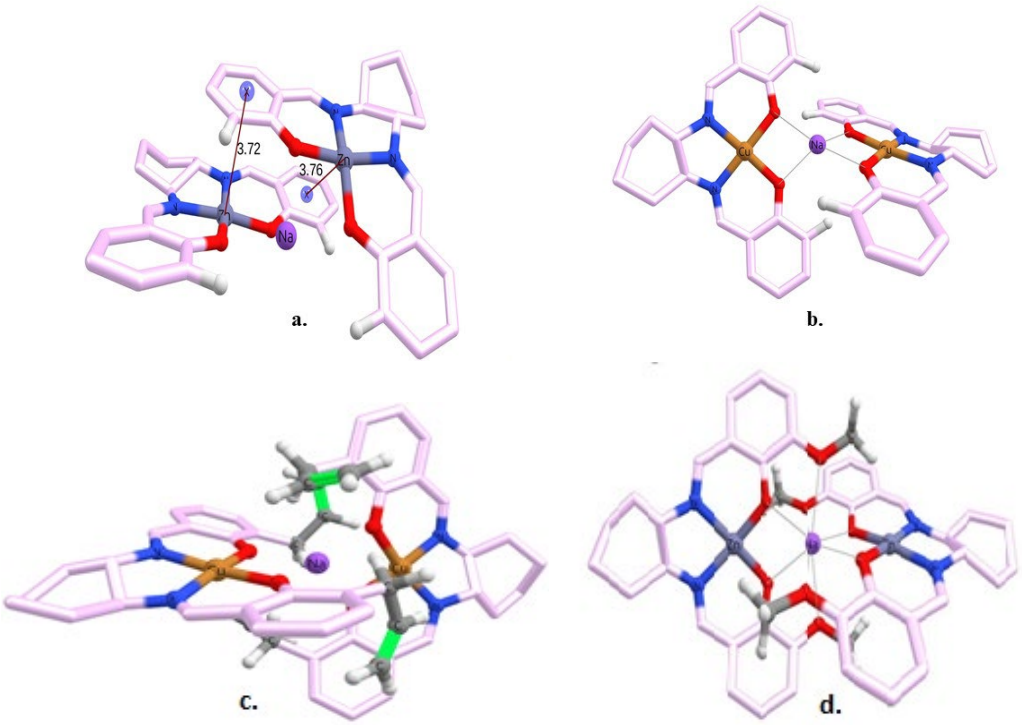

Figure 6. DFT optimized structures of binuclear complexes: **a.** propeller-like structure of unsubstituted Zn(II) complex; **b.** cross-like structure of unsubstituted Cu(II) complex; **c.** propeller-like structure of 3-allylsubstituted Cu(II) complex; **d.** cross-like structure of 3-methoxysubstituted Zn(II) complex.

In the case of the Propeller-like structure, a relatively small change in the Gibbs free energy during dimerization and a relatively large distance between the metal ions are fixed. Such data indicate a low catalytic ability of these salen complexes. In contrast, in the case of the Cross-like structure, the difference in Gibbs free energy between the dimeric and monomeric molecules is relatively large, and the distance between the metal ions is comparatively low. This arrangement of groups in the dimeric structure indicates high catalytic activity of salen complexes.

DFT calculations have shown that in the dimeric structure of 3-allyl-substituted salen complex three out of four molecules have Propeller-like structure. In the dimeric structure of 3-methoxy-substituted salen complex of Zn(II) ion, all particles have Cross-like structure. Cross-like structure was also found in the dimeric structure of the unsubstituted salen complex of Cu(II) ion, but the unsubstituted salen complex of Zn(II) ion predominantly contains Propeller-like structures. Both Propeller-like and Cross-like structural isomers were found in the dimeric structure of other salen complexes, and depending on their ratio, these complexes can be active or passive catalysts.

Thus, the analysis of the DFT-calculation data indicates that Cross-like conformational structures of dimeric salen complexes promote enantioselective catalysis, while Propeller-like structures, on the contrary, inhibit the catalytic ability of the complexes. These data clearly correlate with the experimental data.

Summarizing the obtained data on salen catalysis, it might be stated that indeed in the transition state of alkylation the complex-catalyst takes part in the form of an ionically bound dimeric molecule. Based on these arguments, covalently bound dimeric binuclear salen Cu(II) complexes were synthesized and tested in reaction of alkylation of unsubstituted alanine substrate with benzylbromide, as phase transfer catalyst (*ee*>80%) [31] (Figure 7).

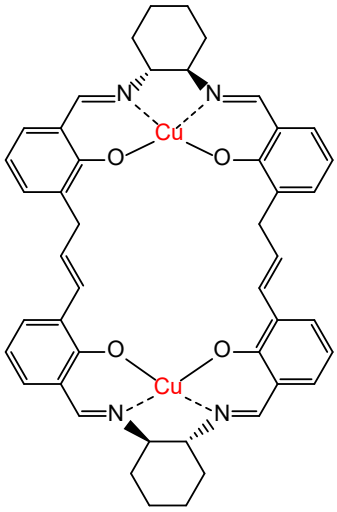

Figure 7. The structure of covalently bound dimeric binuclear salen complexs of Cu(II) ion.

At present, the most promising synthesized salen complexes of Cu(II) and Zn(II) ions are being studied in the alkylation reaction of valine substrates - Schiff bases of isopropyl ester of D,L-valine and substituted benzaldehydes. Importantly, that all previous attempts to alkylate the valine moiety using both stoichiometric and catalytic methods, including phase-transfer salen catalysis, have been unsuccessful [29]. The newly synthesized, the most promising salen complex catalysts are also being investigated in Michael nucleophilic addition reactions to the C=C bond of dehydroalanine analog of O'Donnell's substrate. Research on the synthesis and modification of salen complexes and amino acid substrates, as well as the optimization of phase-transfer catalysis methods is ongoing.

3. Conclusions

The stereodifferentiating ability of salen complexes of Cu(II), Ni(II) and Zn(II) ions, derived from Schiff bases of chiral 1,2-cyclohexyldiamine and substituted salicylaldehydes (PTC), was studied in Cα-alkylation reactions of amino acid substrates — specifically, Schiff bases of the *iso*-propyl ester of D,L-alanine and substituted benzaldehydes.

The chosen alkylating agents were MeI, BnBr, AllylBr and PropargylBr. We found that substituents at the 3-position of the aromatic ring in the salicylidene fragment of the complexes have a particularly strong influence on the stereodifferentiating ability of the catalyst. These findings contribute to a deeper understanding of structure–activity relationships in salen-mediated asymmetric catalysis.

Specifically, it was shown that the allyl substituent strongly inhibits catalytic activity, whereas the methoxy group significantly enhances it. The most efficient catalyst was identified as the 3-methoxy-substituted Zn(II) salen complex, achieving *ee*>90%. DFT calculations demonstrated that the stereodifferentiating ability of the catalyst depends on the ratio of Propeller-like and Cross-like conformational isomers in the dimeric binuclear structure of the salen complex-catalysts in the transition state of the alkylation reaction.

In the dimeric binuclear structure of 3-allyl-substituted salen complexes, the Propeller-like conformational isomers dominate (3/4), which, according to DFT calculations, correspond to a catalytically less active form. In contrast, the dimeric binuclear structures of 3-methoxy-substituted salen complexes that contain only Cross-like conformational isomers according to DFT calculation are catalytically active forms. Depending on the ratio of Propeller-like and Cross-like conformational isomers of the dimeric binuclear structures, a salen complex may act as an active or inactive phase-transfer catalyst. The DFT calculation results correlate clearly with the experimental data. Analysis of the obtained data confirms that the salen complex catalyst participates in the transition state of the

alkylation reaction in the form of ionically bound dimeric binuclear molecules, which served as a basis for the synthesis of covalently linked dimeric binuclear salen complexes with a more rigid intramolecular structure.

4. Experimental and note

4.1. Materials

All reagents were obtained from commercial sources and used without further purification. Thin-layer chromatography (TLC) was carried out on aluminum foil backed sheets precoated with 0.2 mm Kielselgel 60 F254 (Merck, Darmstadt, Germany). The spots were visualized by UV irradiation (λ=254 nm). Column chromatography was performed on Fluka silica gel 60 (0.063–0.200 mm, 70–320 mesh) on a glass column.

4.2. Instrumentation

Melting points (mp) were determined by digital melting point instrument Stuart SMP30 Melting Point (Bibby Scientific Limited, Staffordshire England, UK). NMR spectra were recorded in deuterated solvents using Varian Mercury Vx 300 MHz (USA, Palo-Alto) and BRUKER AVANCE NEO 400 in the case of the 15 compound. Chemical shifts (δ) are reported in parts per million (ppm) relative to tetramethyl silane. Signals were referenced to the residual solvent peak 7.26 (CDCl3), 3.31 (CD3OD), 4.79 (D2O), 2.50 ((CD3)2SO) for 1H and 77.10 (CDCl3), 49.15 (CD3OD), 39.52 ((CD3)2SO) for 13C NMR spectra. The 13C NMR spectra were measured with proton decoupling. Coupling constants are reported in Hertz (Hz). Abbreviations for splitting patterns are as follows: s, singlet; d, doublet; t, triplet; q, quartet; qt, quintet; sext, sextet; hept, heptet; m, multiplet; br., broad. The optical rotation was measured on a Perkin Elmer-341 polarimeter (Waltham, Massachusetts, USA). Elemental analysis was performed by “Euro EA3000” elemental analyzer (Eurovector, Pavia, Italy). For the cation exchange a Dowex-50 (H+ form) column was used. The chromatographic system used to determine the enantiomeric purity of the amino acids was a Waters Alliance 2695e Separation Module HPLC system equipped with PDA detector (Waters Corporation, Milford, Massachusetts, USA). The separation was accomplished in isocratic mode on a Nautilus-E 5μ” 4.0 × 250 mm column (BioChimMac ST Company, Moscow, Russia) at 30 ◦C. The mobile phase consisted of methanol and monosodium phosphate buffer (25 mmol/L). The compounds enantiomeric yield was proved by chiral HPLC analysis of the isolated amino acids. The RAMAN analysis was done by Senterra II Raman Microscope (Bruker, Germany). The IR analysis was done by IR Tracer-100, equipped with GladiATR 10, Shimadzu corporation, Japan and NICOLET AVATAR 330 FT-IR. The asymmetric yield is calculated as the value of three measurements.

4.3. Theoretical calculation methodology

All theoretical calculations were performed in the framework of density functional theory (DFT) using the hybrid functional B3LYP [38] in the ORCA 5.0.3 program [39]. The effect of the solvent was designed using the dielectric polarizable continuum model CPCM [40] with the dielectric constant corresponding to CH2Cl2 solvent, as implemented in ORCA 5.0.3. The optimized geometries were obtained using the def2-TZVP basis set of the Alrich’s def2 family [41] with the def2/J auxiliary set. To calculate the vibrational energy of the resulting def2-TZVP geometries, the basis was retained only for the atoms included in the core of the transition metal complex, i.e. for *Cu/Zn, O, N, Na*, and for the rest of the hydrocarbon core the lighter def2-SVP was used. The dispersion correction to the electronic energy D3BJ was also taken into account according to Grimme, et al. [42]. Computations were performed on the NVIDIA DGX A100 cluster which was acquired by the RA MES State Committee of Science grant project N◦10–3/22Eq-10.

The synthesis of (1*S*,2*S*)-diaminocyclohexane was performed following a previously reported method [43]. The synthesis of salen complexes of Cu(II), Ni(II) and Zn(II) ions, as well as amino acid substrates, was carried out according to previously developed methods [29, 32–33].

References

(1) Izumi, Y.; Chibata, I. Production and Utilization of Amino Acids. *Angew. Chem., Int. Ed.* **1978**, *17*, 176–183. https://doi.org/10.1002/anie.197801761.

(2) Saghyan, A.; Langer, P. Asymmetric Synthesis of Non-Proteinogenic Amino Acids. Wiley-VCH, **2016,** 359pp. https://doi.org/10.1002/9783527804498.

(3) Fik-Jaskółka, M. A.; Mkrtchyan, A. F.; Saghyan, A. S.; et al. Spectroscopic and SEM evidences for G4-DNA binding by a synthetic alkyne-containing amino acid with anticancer activity. *Spectrochim. Acta, Part A* **2020**, *229*, 117884. https://doi.org/10.1016/j.saa.2019.117884.

(4) Palumbo, R.; Simonyan, H.; Roviello, G. N. Advances in Amino Acid-Based Chemistry. *Pharmaceuticals* **2023**, *16*, 1490. https://doi.org/10.3390/ph16101490.

(5) Scognamiglio, P. L.; Riccardi, C.; Palumbo, R.; Gale, T. F.; Musumeci, D.; Roviello, G. N. Self-assembly of thyminyl l-tryptophanamide (TrpT) building blocks for the potential development of drug delivery nanosystems. *J. Nanostruct. Chem.* **2024**, *14*. https://doi.org/10.1007/s40097-023-00523-7.

(6) Hickey, J. L.; Sindhikara, D.; Zultanski, S. L.; Schultz, D. M. Beyond 20 in the 21st Century: Prospects and Challenges of Non-Canonical Amino Acids in Peptide Drug Discovery. *ACS Med. Chem. Lett.* **2023**, *14*, 557–565. https://doi.org/10.1021/acsmedchemlett.3c00037.

(7) Yasser, N.; Mazrou, Y. S. A.; El-Gammal, N. A.; et al. Non-proteinogenic amino acids mitigate oxidative stress and enhance the resistance of common bean plants against *Sclerotinia sclerotiorum*. *Front. Plant Sci.* **2024**, *15*, 1385785. https://doi.org/10.3389/fpls.2024.1385785.

(8) Oeller, M.; Ryan, B. H. L.; et al. Sequence-based prediction of the intrinsic solubility of peptides containing non-natural amino acids. *Nat. Commun.* **2023**, *14*. https://doi.org/10.1038/s41467-023-42940-w.

(9) Simonyan, H.; Palumbo, R.; Petrosyan, S.; et al. BSA Binding and Aggregate Formation of a Synthetic Amino Acid with Potential for Promoting Fibroblast Proliferation: An In Silico, CD Spectroscopic, DLS, and Cellular Study. *Biomolecules* **2024**, *14*, 579. https://doi.org/10.3390/biom14050579.

(10) Wei, L.; Zhu, Q.; Xu, S. M.; Chang, X.; Wang, C. J. Stereodivergent Synthesis of α,α-Disubstituted α-Amino Acids via Synergistic Cu/Ir Catalysis. *J. Am. Chem. Soc.* **2018**, *140*, 1508–1513. https://doi.org/10.1021/jacs.7b12174.

(11) Nowak, M. G.; Skwarecki, A. S.; Milewska, M. J. Amino Acid-Based Antimicrobial Agents—Synthesis and Properties. *ChemMedChem* **2021**, *16*, 3513–3544. https://doi.org/10.1002/cmdc.202100503.

(12) Wang, X.; Yang, X.; Wang, Q.; Meng, D. Unnatural amino acids: promising implications for the development of new antimicrobial peptides. *Crit. Rev. Microbiol.* **2022**. https://doi.org/10.1080/1040841X.2022.2047008.

(13) Szcześniak, P.; Pieczykolan, M.; Stecko, S. The Synthesis of α,α-Disubstituted α-Amino Acids via Ichikawa Rearrangement. *J. Org. Chem.* **2016**, *81*, 1057–1074. https://doi.org/10.1021/acs.joc.5b02628.

(14) Oba, M.; Kunitake, M.; Kato, T.; Ueda, A.; Tanaka, M. Enhanced and Prolonged Cell-Penetrating Abilities of Arginine-Rich Peptides by Introducing Cyclic α,α-Disubstituted α-Amino Acids with Stapling. *Bioconjugate Chem.* **2017**, *28*, 1801–1806. https://doi.org/10.1021/acs.bioconjchem.7b00190.

(15) Wang, C.; Qi, R.; Wang, R.; Xu, Z. Photoinduced C(sp^3)–H Functionalization of Glycine Derivatives: Preparation of Unnatural α-Amino Acids and Late-Stage Modification of Peptides. *Acc. Chem. Res.* **2023**, *56*, 2110–2125. https://doi.org/10.1021/acs.accounts.3c00260.

(16) Wang, Q.; Wang, L. New Methods Enabling Efficient Incorporation of Unnatural Amino Acids in Yeast. *J. Am. Chem. Soc.* **2008**, *130*, 6066–6067. https://doi.org/10.1021/ja800894n.

(17) Yu, Y.; Hu, C.; Xia, L.; Wang, J. Artificial Metalloenzyme Design with Unnatural Amino Acids and Non-Native Cofactors. *ACS Catal.* **2018**, *8*, 1851–1863. https://doi.org/10.1021/acscatal.7b03754.
(18) Ji, P.; Li, J.; Tao, Y.; et al. Direct Asymmetric α-Alkylation of NH_2-Unprotected Amino Acid Esters Enabled by Biomimetic Chiral Pyridoxals. *ACS Catal.* **2023**, *13*, 9150–9157. https://doi.org/10.1021/acscatal.3c01770.
(19) Yamamoto, H.; Ramakrishna, I. Alkylation of Glycine Derivatives to Access Nonnatural Amino Acids. *Synfacts* **2020**, *16*, 1119. https://doi.org/10.1055/s-0040-1705860.
(20) Tsuji, T.; Hashiguchi, K.; Yoshida, M.; et al. α-Amino acid and peptide synthesis using catalytic cross-dehydrogenative coupling. *Nat. Synth.* **2022**, *1*, 304–312. https://doi.org/10.1038/s44160-022-00037-0.
(21) Matsumoto, Y.; Sawamura, J.; Murata, Y.; Nishikata, T.; Yazaki, R.; Ohshima, T. Amino Acid Schiff Base Bearing Benzophenone Imine as a Platform for Highly Congested Unnatural α-Amino Acid Synthesis. *J. Am. Chem. Soc.* **2020**, *142*, 8498–8505. https://doi.org/10.1021/jacs.0c02707.
(22) Noda, H.; Shibasaki, M. Recent Advances in the Catalytic Asymmetric Synthesis of β^2- and $\beta^{2,2}$-Amino Acids. *Eur. J. Org. Chem.* **2020**, 2350–2361. https://doi.org/10.1002/ejoc.201901596.
(23) Cabré, A.; Verdaguer, X.; Riera, A. Recent Advances in the Enantioselective Synthesis of Chiral Amines via Transition Metal-Catalyzed Asymmetric Hydrogenation. *Chem. Rev.* **2021**, *122*, 269–339. https://doi.org/10.1021/acs.chemrev.1c00496.
(24) O'Neil, L. G.; Bower, J. F. Electrophilic Aminating Agents in Total Synthesis. *Angew. Chem., Int. Ed.* **2021**, *60*, 25640–25666. https://doi.org/10.1002/anie.202102864.
(25) Greck, C.; Drouillat, B.; Thomassigny, C. Asymmetric Electrophilic α-Amination of Carbonyl Groups. *Eur. J. Org. Chem.* **2004**, 1377–1385. https://doi.org/10.1002/ejoc.200300657.
(26) Zhang, S.; Li, D.; Wang, B.; et al. Palladium-Catalyzed Asymmetric Trifluoromethylated Allylic Alkylation of N-Substituted Glycine Ethyl Esters with α-(Trifluoromethyl)alkenyl Acetates. *Eur. J. Org. Chem.* **2023**. https://doi.org/10.1002/ejoc.202300593.
(27) Liu, Z.-C.; Wang, Z.-Q.; Zhang, X.; Yin, L. Copper(I)-catalyzed asymmetric alkylation of α-imino esters. *Nat. Commun.* **2023,** *14*, 2187. https://doi.org/10.1038/s41467-023-37967-y.
(28) Belokon, Y. N.; North, M.; Churkina, T. D.; Ikonnikov, N. S.; Maleev, V. I. Chiral salen–metal complexes as novel catalysts for the asymmetric synthesis of α-amino acids under phase transfer catalysis conditions. *Tetrahedron* **2001**, *57*, 2491–2498. https://doi.org/10.1016/S0040-4020(01)00072-2.
(29) Tovmasyan, A. S.; Mkrtchyan, A. F.; Khachatryan, H. N.; et al. Synthesis, Characterization, and Study of Catalytic Activity of Chiral Cu(II) and Ni(II) Salen Complexes in the α-Amino Acid C-α Alkylation Reaction. *Molecules* **2023**, *28*, 1180. https://doi.org/10.3390/molecules28031180.
(30) Hovhannisyan, A. M.; Tovmasyan, A. S.; Mkrtchyan, A. F.; et al. Synthesis and evaluation of new mono- and binuclear salen complexes for the Cα-alkylation reaction of amino acid substrates as chiral phase transfer catalysts. *Mol. Catal.* **2024**, *569*, 114618. https://doi.org/10.1016/j.mcat.2024.114618.
(31) Belokon, Y. N.; Bhave, D.; D'Addario, D.; Groaz, E.; North, M.; Tagliazucca, V. Copper(II)salen catalysed, asymmetric synthesis of α,α-disubstituted amino acids. *Tetrahedron* **2004**, *60*, 1849–1861. https://doi.org/10.1016/j.tet.2003.12.031.
(32) Banti, D.; Belokon, Y. N.; Fu, W. L.; Groaz, E.; North, M. Mechanistic studies on the asymmetric alkylation of amino ester enolates using a copper(ii)salen catalyst. *Chem. Commun.* **2005**, 2707–2709. https://doi.org/10.1039/b500813a.
(33) Mazurek, A.; Szeleszczuk, Ł.; Pisklak, D. M. Periodic DFT Calculations—Review of Applications in Pharmaceutical Sciences. *Pharmaceutics* **2020**, *12*, 415. https://doi.org/10.3390/pharmaceutics12050415.

(34) Liu, S. C.; Zhu, X. R.; Liu, D. Y.; Fang, D. C. DFT calculations in solution systems: solvation energy, dispersion energy and entropy. *Phys. Chem. Chem. Phys.* **2023**, *25*, 913–931. https://doi.org/10.1039/D2CP04720A.
(35) Hirshfeld, F. L. Bonded-atom fragments for describing molecular charge densities. *Theor. Chim. Acta* **1977**, *44*, 129–138. https://doi.org/10.1007/BF00549096.
(36) Trost, B. M.; Xu, J.; Schmidt, T. Palladium-Catalyzed Decarboxylative Asymmetric Allylic Alkylation of Enol Carbonates. *J. Am. Chem. Soc.* **2009**, *131*, 18343–18357. https://doi.org/10.1021/ja9053948.
(37) Sampani, S. I.; Aubert, S.; Cattoen, M.; et al. Dinucleating Schiff base ligand in Zn/4f coordination chemistry: synthetic challenges and catalytic activity evaluation. *Dalton Trans.* **2018**, *47*, 4486–4493. https://doi.org/10.1039/C8DT00538A.
(38) Becke, A. D. Density-functional thermochemistry. I. The effect of the exchange-only gradient correction. *J. Chem. Phys.* **1992**, *96*, 2155–2160. https://doi.org/10.1063/1.462066.
(39) Vosko, S. H.; Wilk, L.; Nusair, M. Accurate spin-dependent electron liquid correlation energies for local spin density calculations: a critical analysis. *Can. J. Phys.* **1980**, *58*, 1200–1211. https://doi.org/10.1139/p80-159.
(40) Neese, F. Software update: The ORCA program system—Version 5.0. *WIREs Comput. Mol. Sci.* **2022**. https://doi.org/10.1002/wcms.1606.
(41) Barone, V.; Cossi, M. Quantum Calculation of Molecular Energies and Energy Gradients in Solution by a Conductor Solvent Model. *J. Phys. Chem. A* **1998**, *102*, 1995–2001. https://doi.org/10.1021/jp9716997.
(42) Weigend, F.; Ahlrichs, R. Balanced basis sets of split valence, triple zeta valence and quadruple zeta valence quality for H to Rn: Design and assessment of accuracy. *Phys. Chem. Chem. Phys.* **2005**, *7*, 3297–3305. https://doi.org/10.1039/B508541A.
(43) Larrow, J. F.; Jacobsen, E. N.; Gao, Y.; Hong, Y.; Nie, X.; Zepp, C. M. A Practical Method for the Large-Scale Preparation of [N,N′-Bis(3,5-di-tert-butylsalicylidene)-1,2-cyclohexanediaminato(2-)]manganese(III) Chloride, a Highly Enantioselective Epoxidation Catalyst. *J. Org. Chem.* **1994**, *59*, 1939–1942. https://doi.org/10.1021/jo00086a062.

Author's Contributions: Anna S. Tovmasyan: Methodology, Investigation. Anna F. Mkrtchyan: Conceptualization, Funding acquisition, Writing—review and editing. Ashot S. Saghyan: Conceptualization, Funding acquisition, Project administration, Resources, Supervision, Writing—original draft, Writing—review and editing.

Funding: Computations were performed on the NVIDIA DGX A100 cluster obtained through grant project No. 10–3/22Eq-10 from the Higher Education and Science Committee of the RA MoESCS. Additional support was provided by joint research projects SCS 21AG-1D013 and ISTC AM-2705 from the same committee.

Informed Consent Statement: Not applicable.

Data and Code Availability Statement: Not applicable.

Acknowledgments: We sincerely thank the Optical Spectroscopy and the NMR Magnetic Resonance Spectroscopy Laboratories of the Scientific Technological Center of Organic and Pharmaceutical Chemistry of the National Academy of Sciences of the Republic of Armenia for their invaluable support in conducting Raman, FTIR, and NMR measurements. We also thank the Analysis Laboratory and the Laboratory of BAS Purification and Certification of the SPC "Armbiotechnology" NAS RA for performing the elemental analysis. Their expertise and access to cutting-edge facilities were instrumental to this work. We are also grateful to Professor Yu. N. Belokon for insightful consultations and guidance throughout the study.

Institutional Review Board Statement: Not applicable.

Conflicts of Interest: The authors declare no conflicts of interest.

Reports of NAS RA
ՀՀ ԳԱԱ Զեկույցներ
NATIONAL ACADEMY OF SCIENCES OF THE REPUBLIC OF ARMENIA
ՀԱՅԱՍՏԱՆԻ ՀԱՆՐԱՊԵՏՈՒԹՅԱՆ ԳԻՏՈՒԹՅՈՒՆՆԵՐԻ ԱԶԳԱՅԻՆ ԱԿԱԴԵՄԻԱ

ԱՄՓՈՓԱԳԻՐ

α-Ամինաթթուների Cα-ալկիլացման մեխանիզմի տարբեր ասպեկտների ուսումնասիրությունը միջֆազային քիրալ սալենային կատալիզատորների պայմաններում

Աննա Ս. Թովմասյան[1,*], Աննա Ֆ. Մկրտչյան[1,2], Աշոտ Ս. Սաղյան[1,2]

[1] «Հայկենսատեխնոլոգիա» ԳԱԿ, Գյուրջյան 14, Երևան 0056, ՀՀ
[2] Երևանի պետական համալսարան, Ալեք Մանուկյան 1, Երևան 0025, ՀՀ

* Հաղորդակցության համար՝ anna.tovmasyan1@edu.isec.am

Անցումային շարքի մետաղների՝ Cu(II), Ni(II) և Zn(II) քիրալ սալենային կոմպլեքսների ստերեոդիֆերենցող հատկությունները ուսումնասիրվել են ամինաթթվային սուբստրատների Cα-ալկիլացման ասիմետրիկ ռեակցիաներում՝ որպես քիրալային կատալիզատորներ: Ստացված արդյունքները ցույց են տվել, որ սալենային կոմպլեքսների կատալիտիկ և ստերեոդիֆերենցող ակտիվությունը զգալիորեն կախված է սալիցիլալդեհիդային հատվածում՝ արոմատիկ օղակի 3-րդ դիրքում գտնվող տեղակալիչի բնույթից: Հետազոտության տվյալների համաձայն՝ առավել բարձր կատալիտիկ արդյունավետություն ցուցաբերել է Zn(II)-ի սալենային կոմպլեքսը, որի սալիցիլիդենային օղակի 3-րդ դիրքում տեղակալված է մեթօքսի խումբ: Այս կոմպլեքսը ցուցաբերել է մինչև 90% կատալիտիկ ակտիվություն: Քիրալ սալենային կոմպլեքսների ստերեոդիֆերենցող ակտիվության մեխանիզմի բացատրության համար իրականացվել են DFT (Density Functional Theory) հաշվարկներ: Ըստ հաշվարկների՝ կատալիզատորների ակտիվությունը պայմանավորված է դիմերիկ երկմիջուկ կառուցվածքով կոմպլեքսների պրոպելլերանման (propeller-like) և խաչաձև (cross-like) կոնֆորմացիոն իզոմերների հարաբերակցությամբ՝ ալկիլացման անցումային վիճակում: Պարզվել է, որ պրոպելլերանման կոնֆորմացիաները, որոնք գերակշռում են արոմատիկ օղակի 3-րդ դիրքում ալիլային խումբ պարունակող սալենային կոմպլեքսներում, համապատասխանում են կատալիտիկ ոչ ակտիվ ձևին և արգելակում են ասիմետրիկ կատալիզը: Իսկ խաչաձև կոնֆորմացիաները, որոնք գերակշռում են 3-րդ դիրքում մեթօքսի խումբ պարունակող անալոգներում, ապահովում են բարձր ստերեոդիֆերենցող ակտիվություն և նպաստում են արդյունավետ ասիմետրիկ կատալիզին: DFT հաշվարկներով ստացված արդյունքները համընկնում են փորձարարական տվյալների հետ:

Բանալի բառեր՝ ոչ սպիտակուցային ամինաթթուներ, քիրալային կատալիզատորներ, ասիմետրիկ կատալիզ, սալենային կոմպլեքսներ, ստերեոսելեկտիվություն